



Published in final edited form as:

Circ Res. 2021 July 23; 129(3): 435–450. doi:10.1161/CIRCRESAHA.120.318601.

Activation of Autophagic Flux Blunts Cardiac Ischemia/Reperfusion Injury

Min Xie^{#1}, Geoffrey W. Cho^{#1}, Yongli Kong¹, Dan L. Li¹, Francisco Altamirano¹, Xiang Luo¹, Cyndi R. Morales¹, Nan Jiang¹, Gabriele G. Schiattarella¹, Herman I. May¹, Jessica Medina¹, John Shelton¹, Anwarul Ferdous¹, Thomas G. Gillette¹, Joseph A. Hill^{1,2}

¹Department of Internal Medicine (Cardiology), University of Texas Southwestern Medical Center, Dallas, Texas 75235, USA

²Department of Molecular Biology, University of Texas Southwestern Medical Center, Dallas, Texas 75235, USA

These authors contributed equally to this work.

Abstract

Rationale: Reperfusion injury accounts for up to half of myocardial infarct size, and meaningful clinical therapies targeting it do not exist. We have reported previously that autophagy is reduced during reperfusion and that HDAC inhibition enhances cardiomyocyte autophagy and blunts ischemia/reperfusion (I/R) injury when administered at the time of reperfusion. However, whether inducing autophagy *per se*, as opposed to other effects triggered by HDAC inhibition, is sufficient to protect against reperfusion injury is not clear.

Objective: We set out to test whether augmentation of autophagy using a specific autophagy-inducing peptide, Tat-Becn1, protects the myocardium through reduction of reactive oxygen species (ROS) during reperfusion injury.

Methods and Results: Eight to twelve-week-old, wild-type, C57BL6 mice and drug-inducible cardiomyocyte-specific ATG7 knockout mice (to test the dependency on autophagy) were randomized into two groups: exposed to a control Tat-Scrambled (TS) peptide or a Tat-Becn1 (TB) peptide. Each group was subjected to I/R surgery (45min coronary ligation, 24h reperfusion). Infarct size, systolic function, autophagic flux, and ROS were assayed. Cultured neonatal rat ventricular myocytes (NRVMs) were exposed to TB during simulated ischemia/reperfusion injury. ATG7 knockdown by siRNA in NRVMs was used to evaluate the role of autophagy. TB treatment at reperfusion reduced infarct size by 20% (absolute reduction; 50% relative reduction) and improved contractile function. Improvement correlated with increased autophagic flux in the border zone with less oxidative stress. ATG7 KO mice did not manifest TB-promoted

Address correspondence to: Dr. Joseph A. Hill, Division of Cardiology, UT Southwestern Medical Center, NB11.200, 6000 Harry Hines Blvd, Dallas, TX 75390-8573, Tel: 214.648.1400, joseph.hill@utsouthwestern.edu.

Publisher's Disclaimer: This article is published in its accepted form. It has not been copyedited and has not appeared in an issue of the journal. Preparation for inclusion in an issue of *Circulation Research* involves copyediting, typesetting, proofreading, and author review, which may lead to differences between this accepted version of the manuscript and the final, published version.

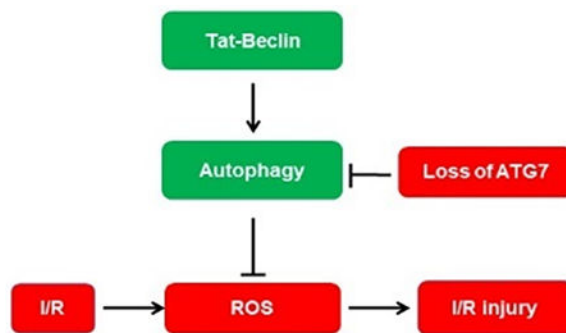
DISCLOSURES

All authors have reported no conflicts of interest.

cardioprotection during I/R. In NRVMs subjected to I/R, TB reduced cell death by 41% and reduced I/R-induced ROS generation. Conversely, ATG7 knockdown in NRVMs abolished these beneficial effects of TB on cell death and ROS reduction.

Conclusions: Induction of autophagy at the time of reperfusion is sufficient to mitigate myocardial reperfusion injury by reducing ROS and cell death. Maintenance of appropriate autophagic flux may emerge as a viable clinical therapy to reduce reperfusion injury in acute myocardial infarction.

Graphical Abstract



Keywords

Ischemia/reperfusion; cardiomyopathy; autophagy; histone deacetylase; reactive oxygen species; ischemia reperfusion injury; Beclin; Chronic Ischemic Heart Disease; Heart Failure; Myocardial Infarction

INTRODUCTION

Ischemic heart disease is the leading cause of death worldwide, resulting in the death of over 7 million people each year¹⁻³. Standard treatments for acute coronary syndromes (ACS), such as interventions to decrease oxygen demand coupled with restoration of blood flow in the infarct-related artery, target the ischemic phase of injury^{4,5}. However, the sudden change from an anoxic to normoxic milieu has been demonstrated to contribute significantly to myocardial damage^{6,7}. Indeed, this so-called reperfusion injury can account for up to 50% of final infarct size^{8,9}. Yet, despite the magnitude of this injury response, there are currently no efficacious therapies in clinical use targeting the reperfusion phase of the ischemia/reperfusion (I/R) injury process^{8,10-12}.

We and others have demonstrated that inhibition of class I histone deacetylases (HDACs) at the time of reperfusion confers robust cardioprotection in multiple animal models of I/R injury¹³⁻¹⁹. Our previous work demonstrated that HDACi (HDAC inhibition) promotes cardiomyocyte autophagy^{15,19-22}. Autophagy, an evolutionarily conserved process of intracellular protein degradation and recycling, plays a critical role in the cardiomyocyte response to stress^{16,23-25}. Our work pointed to a requirement for induction of cardiomyocyte autophagy in the protection against reperfusion injury afforded by HDACi^{15,19,22,26}. However, as HDACs govern a wide range of cellular processes and their

small molecule inhibitors may have off-target effects, we set out to modulate cardiomyocyte autophagy directly in a manner that does not involve altering HDAC activity to test whether induction of autophagic flux *per se* is sufficient to afford protection from reperfusion injury²⁷.

METHODS

Data Availability.

The authors will make their data, analytic methods, and study materials available to other researchers based on reasonable request. Please see the Major Resources Table in the Supplemental Materials.

Animals.

For I/R surgeries, 8 to 12-week-old C57BL6 wild-type mice were utilized. Concurrently, ATG7 KO (α MHC-mer-Cre-mer) mice were available in the Hill Lab at UT Southwestern. All experiments were performed with male mice, as female mice manifest less myocardial infarction injury in the setting of ischemia-reperfusion²⁸. Mice were anesthetized with 2.4% isoflurane and placed supine on a heating pad (37°C). Animals were intubated (19G stump needle) and ventilated with room air using a MiniVent mouse ventilator (Hugo Sachs Elektronik; stroke volume, 250 μ L; respiratory rate, 210 breaths per minute). Following left thoracotomy (between the 4th and 5th ribs), the left anterior descending coronary artery was visualized under a dissecting microscope (Leica) and ligated with a 6-0 Prolene suture. Regional ischemia was confirmed by visual inspection with the same microscope by observing discoloration of the myocardium distal to the occlusion. After 45 minutes of ischemia, the ligation was then released and the tissue allowed to reperfuse as confirmed by visual inspection. All procedures were approved by the University of Texas Southwestern Medical Center Institutional Animal Care and Use Committee. Mice were fed standard rodent chow (Harlan Teklad 2016 standard chow; 12% kcal fat; 3.0 kcal/g) at all times before and after surgeries.

2,3,5-triphenyltetrazolium chloride staining.

At the time of anesthesia and again before euthanasia, mice were administered heparin 1000 U/kg for anticoagulation to ensure proper dye perfusion. The heart was excised and perfused with phosphate-buffered saline solution (PBS, 5 mL) through an aortic cannula (fitted with a suture to seal the aorta around the cannula). To delineate the occluded-reperfused coronary vascular bed, the coronary artery was then tied at the previous occlusion location, and the aortic root was perfused with a 5% solution of phthalo blue dye in normal saline (5 mL over 5 minutes). Utilizing this method, the portion of the LV supplied by the previously occluded coronary artery (area at risk) was identified by the absence of blue dye, whereas the rest of the LV was stained dark blue.

Atrial and right ventricular tissues were excised. Subsequently, the LV tissue was frozen and cut into 7 slices. To delineate infarcted from viable myocardial tissue, heart slices were incubated with a 1% solution of 2,3,5-triphenyltetrazolium chloride in phosphate buffer (pH 7.4 at 37°C, 5 mL per heart) for 40 minutes. Heart slices were fixed in 10% neutral buffered

formaldehyde, and 24 hours later were weighed and photographed digitally. With this procedure, the nonischemic portion of the LV was stained dark blue, viable tissue within the region at risk was stained bright red, and infarcted tissue was white or light yellow. Image analysis of the samples was performed using ImageJ, and from these measurements, infarct size was calculated as a percentage of the region at risk using standard methods described previously¹⁵. To harvest samples for molecular biological analysis, hearts were cut into the ischemic, border and remote zone with scissors and forceps under a dissecting microscope.

Neonatal cardiomyocyte isolation and culture.

Neonatal rat ventricular myocytes (NRVM) were isolated from postnatal day 1-2 Sprague-Dawley rat pups using the Cellutron Neomyt kit (ThermoFisher, NC-6031). Cell purity was greater than 90% cardiomyocytes. These cells were plated to enrich for cardiac myocytes at a density of $\approx 1,200$ cells/mm² and cultured for 24 hours in DMEM/M199 (3:1 ratio) containing 5% FBS, 10% horse serum, and 100 μ M BrdU (Sigma-Aldrich).

Adult mouse cardiomyocyte isolation.

Adult mouse ventricular cardiomyocytes were harvested as described previously^{15, 29}. Briefly, after retrograde perfusion with Krebs-Ringer solution (2 mL/min for 5 minutes), hearts were perfused with fresh solution containing 0.8 mg/mL collagenase (Worthington type II) for 15 minutes. The LV was then removed and cut into small pieces in KB solution (10 mM taurine; 70 mM glutamic acid; 25 mM KCl; 10 mM KH₂PO₄; 22 mM glucose; 0.5 mM EGTA, pH 7.2). Cells were then filtered and maintained in KB buffer for subsequent use. All isolation steps were carried out at 37°C with continuous gas supply (95% O₂ and 5% CO₂). Gradual calcium re-introduction was performed and cells were plated onto Matrigel (Corning, E1270)-coated plates. Only Ca²⁺-tolerant, rod-shaped cardiomyocytes with typical cross striations were utilized. Cell purity was greater than 98% cardiomyocytes.

Echocardiography.

Echocardiogram recordings were performed on conscious, gently restrained mice utilizing a Vevo 2100 system (MS400C probe). The sonographers were blinded to treatment group assignment. Left ventricular end-diastolic and end-systolic dimensions (LVEDD and LVESD) were derived from M-mode images. FS was calculated as (LVEDD - LVESD)/LVEDD and expressed as a percentage. All measurements were made at the level of the papillary muscles as per standard protocols.

Adenovirus-mediated gene transfer.

Cells were infected 2 days post plating with adenovirus expressing RFP-GFP-tagged LC3 (generated in the Hill Lab at UT Southwestern) at a multiplicity of infection (MOI) of 15 PFU/cell. Afterwards, cells were cultured for an additional 24 hours in DMEM/M199 (3:1) with 3% FBS and then harvested in MPER buffer (Thermo Scientific) containing phoSTOP and protease inhibitor cocktail (Roche).

Tat-Beclin and Tat-Scramble peptides.

Tat-Beclin 1, YGRKKRRQRRRGGTNVFNATFEIWHDGEFGT and Tat-Scrambled, YGRKKRRQRRRGGVGNDFFINHETTGFATEW were synthesized by the UT Southwestern Protein Chemistry and Technology Center, and HPLC purified with a grade >95%. The dilution and storage methods were as previously described³⁰.

Measurement of autophagic flux in mice and NRVMs.

Mice harboring an RFP-GFP-LC3 transgene driven by a CAG promoter were generated by the Hill Lab. Mice were randomly assigned to 3 groups. Control groups received vehicle, dimethyl sulfoxide (DMSO) or Tat-Scramble (20 mg/kg IP ×1); one group received SAHA (suberanilohydroxamic acid, 100 mg/kg SQ ×1); and the last group received Tat-Beclin (20 mg/kg IP ×1). The mice were subjected to 45 minutes of ischemia and 2 hours of reperfusion. Green fluorescent protein (GFP) and red fluorescent protein (RFP) signals were detected in frozen sections by confocal microscopy.

Simulated I/R in cultured cells and assays of cell death and protein oxidation.

For simulated ischemia/reperfusion (sI/R) in NRVMs, cell culture medium was exchanged with an ischemia-mimetic solution (in mmol/L: 20 deoxyglucose, 125 NaCl, 8 KCl, 1.2 KH₂PO₄, 1.25 MgSO₄, 1.2 CaCl₂, 6.25 NaHCO₃, 5 sodium lactate, 20 HEPES, pH 6.6), and the culture plates were placed inside a humidified gas chamber equilibrated with 95% N₂ and 5% CO₂. After 5 hours of simulated ischemia, reperfusion was then initiated by buffer exchange to normoxic NRVM culture medium with 1% fetal bovine serum and incubation in 95% room air and 5% CO₂. Controls incubated in normoxic NRVM culture medium with 1% fetal bovine serum were prepared in parallel. Cell death was detected using the CytoTox 96 Non-Radioactive Cytotoxicity Assay (G1781, Promega) or Cell Luminescence Assay (CellTiter-Glo® Assay based on ATP level, G7570, Promega). Protein oxidation was determined by separate assays (Protein Carbonyl Content Assay Kit MAK094-1KT - Sigma; Oxyblot Protein Oxidation Detection Kit S7150 - Millipore; Protein Carbonyl Colorimetric Assay Kit 10005020 – Caymen Chemical).

For ARVMs, Tat-Beclin or Tat-Scramble was added at the time of reperfusion for a total of 2 hours of treatment, with sI/R total being 2 hours of ischemia and 2 hours of reperfusion. LC3 Western blots were performed to assay levels of autophagy. ARVM death was evaluated by microscopy. Each group was studied in triplicate, and two representative views were examined for each sample with four repeats, such that each group comprised a total 24 readings.

Western blotting.

BioRAD SDS/PAGE gels (4-20%) were run under 150V for 1 hour, transferred to nitrocellulose membranes, and then immunoblotted. Antibodies were purchased from Cell Signaling Technology or Sigma-Aldrich, except for LC3-II (rabbit anti-LC3 prepared in Hill Laboratory at UT Southwestern), ATG7 (Anaspec 54231 and Cell Signaling 2631), and GAPDH (Fitzgerald 10R-G109a). Blots were scanned and quantified using an Odyssey LI-COR (version 3.0) imaging system.

Pharmacological inhibitors and siRNA.

SAHA and bafilomycin-A were purchased from LC Laboratory (V-8477, B-1080 respectively). Tat-Scramble and Tat-Beclin peptides were synthesized in the UT Southwestern Peptide Synthesis Core with the help of Dr. Haydn Ball. All siRNAs were acquired from Sigma-Aldrich.

siRNA knockdown.

NRVMs were isolated and seeded at a density of 1.2 million/well in a 6-well dish. Twenty-four hours after plating, cardiomyocytes were incubated with small interfering RNA (siRNA) negative control (Neg, SIC001), siRNAs targeting ATG7 (SASI_Rn01_00050326 and SASI_Rn01_00050327), each from Sigma and used according to the manufacturer's recommended protocols. In brief, siRNAs were reconstituted into a 40 mmol/L stock solution. Three microliters of the siRNA stock and 3 μ L of RNAiMax transfectant were mixed together (1:1 ratio) in 1 mL of Opti-MEM medium. Cardiomyocytes were incubated with the siRNA master solution for 8 hours, followed by the addition of 1 mL of culture medium containing 1% serum. Twenty-four hours after the siRNA incubation, the cardiomyocytes were utilized for I/R experimentation.

RNA isolation, reverse transcription, and quantitative PCR analysis.

All heart tissue was harvested and then flash frozen immediately in liquid nitrogen and stored at -80°C until use. Quick-RNA Microprep kit was employed according to the manufacturer's recommendations (Zymo Research R1050) for total RNA isolation. 1 μ g RNA from each sample was then used for reverse transcription using the iScript cDNA synthesis kit (Bio-Rad). cDNA was then diluted by 10 using distilled H_2O and used for quantitative PCR analysis (Roche).

Histology.

Heart tissue fixation was accomplished with 4% paraformaldehyde (PFA), then washed and transferred into $1\times$ PBS, followed by paraffin embedding or cryoembedding after sucrose infiltration for immunofluorescence staining. Images were acquired via confocal microscopy (TCS SP5; Leica) with Leica LAS AF software. HC PL APO $20\times/0.70$, HCX PL APO $40\times/1.25-0.75$ oil, and HCX PL APO $63\times/1.40-0.60$ oil lenses were used. Images were then uploaded in ImageJ for analysis. For ideal image capture (optimal brightness/contrast), images were linearly and uniformly scaled without altering, masking, or eliminating data.

Statistics.

Averaged data are expressed as mean \pm SEM. Number per group and *P* values are provided with each figure. Data normality was examined using the Shapiro-Wilk test (with $\alpha=0.05$) and by visual inspection of normal Q-Q plots to ensure that there were no significant deviations from normality. Normally distributed data analyzed by Student's unpaired, 2-tailed *t*-test were used for two-group analysis. One-way ANOVA followed by Tukey's post-hoc multicomparison test was used for multiple group analysis. For non-normally distributed data, the Mann-Whitney test was used for two-group analysis, and the Kruskal-Wallis test with Dunn's multiple comparisons was used for multiple-group analysis. For statistical

comparisons, a *P* value less than 0.05 was considered significant. All statistical analyses were performed using GraphPad Prism (version 8) software with post-hoc multiple testing correction when applicable. We only excluded animals that died or with apparent failure of TTC staining. We calculated the number of animals required based on a prior study with an average of infarct size/area at risk of 40% with a standard deviation of 10% and a 50% infarct size reduction. With $\alpha=0.05$ and 80% power, we required at least 5 analyzable mice in each group to achieve a significant difference.

Study approval.

All studies were approved by the Institutional Animal Care and Use Committee of University of Texas Southwestern Medical Center.

RESULTS

Tat-Beclin rescues cardiac I/R injury in vivo and in vitro.

Prior work from our lab implicated HDACi-dependent activation of autophagic flux in the cardioprotective response elicited by HDAC inhibitors¹⁵. As reversible protein acetylation governed by HDACs is involved in a wide range of cellular events, we set out here to modulate autophagic flux in a manner independent of HDACs. First, we determined whether delivery of a Beclin peptide, rendered cell-permeable by the HIV-derived Tat peptide, is capable of activating autophagy in cardiomyocytes. As expected based on findings from other cell types³⁰, Tat-Beclin treatment increased levels of autophagy as assessed by the autophagy marker LC3-II (Online Figure IA, IB). The response was dose-dependent in both cardiomyocytes and in other cell types (Online Figure IC, Online Figures IIA). Cell death assays were employed to identify an effective dose that induces robust autophagy without provoking toxicity (Online Figure IIB).

To assess the efficacy of autophagic stimulation in the rescue of reperfusion injury *in vivo*, mice were subjected to an established protocol of surgical I/R, one in which the animals received one of 3 randomized/blinded interventions at the time of reperfusion (Tat-Beclin, Tat-Scramble, or vehicle). Subsequently, ventricular contractile function was assessed, and infarct area evaluated (Figure 1A). The two control arms (Tat-Scramble, vehicle) demonstrated no significant difference from each other in terms of changes in I/R injury measured via TTC staining for infarct size (Figures 1B, 1C). However, the Tat-Beclin-treated animals displayed an absolute 20% reduction and a relative 50% ($p<0.05$) reduction in infarct size compared to controls (Figure 1B, 1C). Importantly, areas at risk for infarction were equivalent across all three groups, indicative of the similarity of the surgical procedure (Figure 1B).

To evaluate the functional implications of the diminished infarct size, we evaluated contractile performance by echocardiography. Consistent with decreased infarct size, Tat-Beclin-treated animals manifested a significant improvement in contractile performance, quantified as % fractional shortening of the left ventricle, compared with Tat-Scramble or vehicle-treated groups, the latter two of which were not significantly different from each other (Figures 1D, 1E, Online Figure VIA).

To begin to tease out underlying mechanisms, we turned to an *in vitro* model of simulated I/R (Figure 2A). We confirmed that Tat-Beclin's ability to induce autophagy in cardiomyocytes is dose dependent, as has been shown in other cell types³⁰ and importantly that there appears to be a narrow therapeutic window in which Tat-Beclin is able to reduce I/R injury while stimulating autophagy (Online Figure IIB). In our hands, 2.5 μ M Tat-Beclin had the least toxic effect and afforded the greatest protection from cardiomyocyte I/R injury.

NRVMs were exposed to a paradigm of simulated I/R, and therapeutic intervention was administered at the time of reperfusion, after which cell death was evaluated. As an additional control, the HDAC inhibitor SAHA was used, which we have shown previously to afford cardioprotection in an mTOR-dependent manner^{15, 22}. In contrast with the lack of effect on cell death under control conditions (Figure 2B), we observed a striking reduction in cell death as assed by LDH assay in the group treated with SAHA (Figure 2B). Treatment of the cells with the autophagy-inducing Tat-Beclin peptide provided a similarly significant degree of protection against sI/R-induced cell death (Figure 2B). These results were corroborated using a cell luminescence cell death assay (Online Figure IIC). Similar results were observed in studies of ARVMs (Figure 2C), where Tat-Beclin treatment led to a decrease in cell death of adult cardiomyocytes during reperfusion. Together, these data show that treatment with an autophagy-inducing peptide can protect against I/R-induced cardiomyocyte death, supporting a model in which induction of autophagic flux in cardiomyocytes during reperfusion injury is protective.

Tat-Beclin rescue of cardiac I/R injury requires autophagy.

To evaluate the role of autophagic flux in Tat-Beclin-dependent cardioprotection, we targeted the autophagic pathway by siRNA knockdown of the essential autophagy gene ATG7 (Figure 3A). As before, experimental interventions were imposed in NRVMs at the time of reperfusion with subsequent cell death assessed by LDH efflux. Using bafilomycin (BFA) to assess increases in autophagic flux, we observed that Tat-Beclin's ability to induce autophagy was abolished by ATG7 knockdown (Figure 3A). In siRNA-transfected cells exposed to I/R, Tat-Beclin afforded significant reduction in cardiomyocyte death (Figure 3B). In contrast, Tat-Beclin-dependent rescue of I/R-induced cardiomyocyte death was blocked in NRVMs depleted of ATG7 (Figure 3B).

To evaluate the role of cardiomyocyte autophagy *in vivo*, we turned to a mouse model engineered to be selectively deficient of the essential autophagy factor ATG7 exclusively in cardiomyocytes^{31, 32}. We verified ~80% declines in ATG7 in adult mouse cardiomyocytes by qRT-PCR after 5 days of tamoxifen (20mg/kg IP) treatment (Figure 4A) and by Western blot analysis (Figure 4A). As expected, LC3-II levels were reduced significantly with the loss of ATG7 (Figure 4A). We randomized littermate control (ATG7^{F/F}) and cardiomyocyte-restricted ATG7 knockout (ATG7 KO) mice to the surgical I/R protocol described above. At the time of reperfusion, animals were injected with Tat-Beclin or Tat-Scramble peptide. Throughout, all investigators were blinded to treatment group. As expected, administration of Tat-Scramble conferred no rescue of cardiac infarct size in either ATG7 group (ATG7^{F/F} or KO). Additionally, in agreement with our observations in WT animals (Figures 1A–B), ATG7^{F/F} mice treated at the time of reperfusion with Tat-Beclin manifested significant

decreases in infarct size (Figures 4B, 4C). In the ATG7 KO group, however, Tat-Beclin did not afford rescue from I/R injury (Figures 4B, 4C), lending additional credence to a model in which activation of autophagic flux is required for the cardioprotective response of Tat-Beclin peptide.

To test for functional implications, we evaluated ventricular size and function by echocardiography. Here, we observed partial rescue of the I/R-driven decreases in contractile performance in the animals exposed to Tat-Beclin (Figures 4D, 4E, Online Figure VIB). However, this cardioprotective response was abolished in ATG7 KO mice (Figures 4D, 4E, Online Figure VIB). These data strongly support a model in which induction of autophagy during reperfusion is protective against reperfusion-induced cardiac cell death.

Tat-Beclin rescue of cardiac I/R injury occurs independently of mTOR inhibition.

Mechanistic target of rapamycin (mTOR) is a potent inhibitor of autophagy in normoxic, nutrient-replete conditions.^{22, 33–35} Inhibition of mTOR either pharmacologically or under conditions of starvation results in an increase in autophagy.^{22, 33} We have reported that HDACi stimulation of autophagy occurs through TSC1/2 complex-driven down-regulation of mTOR activity^{7, 22}. Interestingly, both HDAC inhibitors and rapamycin appear to protect against I/R injury^{15, 36}. In contrast, Tat-Beclin induction of autophagy involves the Tat-Beclin peptide competing with endogenous Beclin-1 for binding to the intracellular negative regulator of autophagy, Golgi-associated pathogenesis-related protein 1 (GAPR-1)³⁰. This would suggest that Tat-Beclin acts to stimulate autophagy in an mTOR-independent manner. However, since Tat-Beclin is a peptide and may have pleiotropic effects, we tested this by examining several proteins directly related to the mTOR signaling cascade. First, we noted that Tat-Beclin treatment increased autophagic flux as measured by increased LC3-II, but yet had no effect on mTOR phosphorylation (indirect marker of its activation) or its downstream targets S6 or 4EBP1 (Online Figure IIIA). By contrast, exposure to SAHA triggered similar degrees of autophagy activation (Online Figure IIIB) and elicited significant decreases in mTOR activity, in contrast to the actions of Tat-Beclin (Online Figures IIIB, IIIC). Indeed, this was the case in both normoxic and I/R conditions (Online Figure IIIC). During normal cardiomyocyte function, autophagy is preserved (Online Figures IVA–D), but in I/R conditions, we observed a loss of autophagic flux as demonstrated by lack of LC3-II accumulation in the BFA-treated control groups (Online Figure VA). However, treatment with either SAHA or Tat-Beclin triggered restoration of autophagy as assessed by the renewal of dynamic increases in LC3 levels with BFA administration (Online Figures VA, VB). In aggregate, these data suggest that Tat-Beclin-dependent rescue of I/R injury takes place by stimulation of autophagic flux in an mTOR-independent manner.

Induction of autophagy reduces sI/R-induced oxidative stress.

A large literature points to reactive oxygen species (ROS) and oxidative stress as significant contributors to cardiac damage during reperfusion^{37–39}. In fact, it has been suggested that ROS confer the majority, up to 85%, of the pathological factors that lead to cardiomyocyte cell death during reperfusion injury^{7, 39, 40}. To begin to dissect the cardioprotective mechanisms of autophagic flux during reperfusion, we returned to the *in vitro* NRVM model. As above, we exposed cells to sI/R in the presence of the Tat-Scramble (control) or

autophagy-inducing Tat-Beclin peptide. We then measured the extent of oxidative stress under these conditions by assaying protein carbonylation, an oxidative modification triggered by ROS^{7, 39, 41}. Protein carbonylation was detected using two independent assays, one involving a colorimetric readout and the other involving immunoblot detection. Both assays revealed significant increases in protein carbonylation in cells exposed to s/I/R conditions (Figures 5A, 5B). In contrast, however, treatment of the cells with Tat-Beclin resulted in a significant decrease in s/I/R-induced protein oxidation (Figures 5A, 5B). Treatment with SAHA, which also induces autophagy under these conditions, yielded results similar to Tat-Beclin peptide (Figures 5A, 5B, 5C). Together, these data support a model in which autophagy protects against reperfusion injury by reducing oxidative damage.

Tat-Beclin treatment during reperfusion induces autophagy and decreases oxidative damage in the infarct border zone.

Our previous work suggested that increased autophagic flux in the infarct border zone of the heart is critical to HDACi rescue of I/R injury¹⁵. However, given that Tat-Beclin stimulates autophagy differently, in an mTOR-independent manner, we sought to evaluate whether the effects of Tat-Beclin in I/R injury rescue take place in the border region of infarcted cardiac muscle. We subjected WT mice to the established I/R surgery protocol. After 4 hours of reperfusion, we isolated the hearts, separated the tissue by the zones affected (infarct, border, remote) and analyzed autophagic markers. As we have reported previously¹⁵, steady state LC3-II levels were lower in the infarct and border region of the heart, as compared with the remote region (Figure 6A). Additionally, in agreement with our earlier findings, HDACi treatment increased steady state levels of LC3-II in the border region (Figure 6A). Importantly, we observed a similar increase in steady state levels of LC3-II in the border zone of hearts treated with Tat-Beclin peptide, suggesting that activation of autophagy within the border area accounts for the decrease in cell death in this region (Figure 6A).

To test this idea independently, we turned to a tandem fluorescence (α MHC-RFP-GFP-LC3) reporter mouse line. These mice allow for direct measurements of both autophagosomes (GFP/RFP puncta with yellow fluorescence) and autolysosomes, an organelle in which GFP fluorescence is quenched by the acidic pH milieu (red fluorescence). These mice were subjected to I/R surgery, and the hearts were isolated and sectioned for fluorescence microscopy. In these experiments, we observed that Tat-Beclin injection led to an increase in red punctum formation in the area of infarction, consistent with an increase in autophagosomes and bona fide flux through the autophagosome-lysosome pathway (Figures 6B, 6C).

As an additional control, we returned to the ATG7^{F/F} and ATG7 KO mice. These animals were subjected to I/R surgery followed by exposure Tat-Beclin or control Tat-Scramble peptide. Afterward, ventricular tissue was separated into the affected zones affected (infarct, border, remote) and analyzed. We observed that Tat-Beclin led to increases in steady-state LC3-II levels within the infarct border zone of ATG7^{F/F} mice (Figure 7A). However, Tat-Beclin-induced increases in autophagic flux in the infarct border zone were absent in ATG7 KO mice (Figures 7A, 7B) correlating with blunted rescue of cardiac function and infarct

size (Figures 3A, 3B). In addition, these data also confirm that the increases in autophagic flux are cardiomyocyte-specific.

Our *in vitro* data point to reduced oxidative stress occurring as a result of autophagic flux activation. To test this *in vivo*, we probed these same extracts for evidence of oxidative stress. We observed an increase in protein carbonylation in both the infarct and border zones of the hearts of both genotypes undergoing I/R surgery (Figure 7C). However, the extent of oxidative damage was significantly reduced in the border zone of Tat-Beclin-treated ATG7^{F/F} hearts, a response lost in the ATG7 KO hearts exposed to Tat-Beclin peptide (Figures 7A, 7B, 7C). In aggregate, these data support a model in which increasing autophagic flux during reperfusion injury reduces oxidative stress leading to increased cell survival and decreased infarct size.

DISCUSSION

Our previous work supported a model in which induction of cardiomyocyte autophagy at the time of tissue reperfusion reduces cell death^{15, 22}. In the present study, we set out to confirm and extend these findings and to parse the effects of direct autophagic activation using Tat-Beclin peptide from the more widespread effects of HDAC inhibition. Using this approach, we sought to clarify three important questions. Can an agent that directly activates autophagy reduce I/R injury? If reduction of I/R injury occurs, is the rescue due primarily to changes in autophagic flux? If so, what are the mechanisms underlying the cytoprotective effects of autophagic activation?

Reperfusion injury is a therapeutic target to reduce infarct size during myocardial infarction.

Approximately half of cardiomyocyte death occurs at the time of reperfusion injury. However, despite having been discovered more than 50 years ago, there is currently no standard therapy to reduce reperfusion injury¹². Designing novel therapies for reperfusion injury is therefore of major clinical importance⁸. Whereas the triggers of reperfusion injury occur very rapidly after reperfusion, a number of findings suggest that the ensuing cell death occurs over time such that activation of pro-survival pathways, such as autophagy and the unfolded protein response, confer benefit^{15, 16, 23, 25, 26, 42}. Mechanisms underlying this cell death are several, from cell swelling and rupture that can occur acutely upon reperfusion, to cell death occurring via necrotic, apoptotic, or necroptotic pathways^{7, 40, 43}. Central to this is a change in oxidative status that provokes mitochondrial dysfunction and oxidative damage^{7, 12, 39, 40, 43}.

Maintaining autophagic flux has emerged as an effective protective mechanism of cardiac reperfusion injury.

Autophagy is an intracellular process responsible for the turnover of cellular constituents. An important role of autophagy in I/R injury has been reported, showing that activation of autophagy during reperfusion reduces infarct size^{44, 45}. We reported that an FDA-approved HDAC inhibitor, Suberoylanilide Hydroxamic Acid (SAHA, Vorinostat (Zolinza®, Merck), reduces infarct size by 40% when administered at the time of reperfusion in rabbits, acting

through induction of autophagic flux¹⁵. However, there are pleiotropic effects of HDAC inhibition other than inducing autophagy. To further delineate the role of autophagy during reperfusion injury, we report here that Tat-Beclin peptide delivered at the moment of post-ischemic myocardial reperfusion reduces infarct size and the associated decline in ventricular contractile performance.

Another limitation of this study is that we used fractional shortening (FS) to measure ventricular contractile performance, which might not correlate with left ventricular ejection fraction measured by 3D ECHO⁴⁶. As noted, sonographers were blinded entirely to treatment group assignment. Given that we performed LAD coronary ligation, we consistently measured at the mid papillary muscle level with the M mode line running across the anterior wall and the posterior wall to detect anterior wall hypokinesis, which is the major focus of these biological events. Furthermore, our observations of improved FS and improved left ventricular end-diastolic and end-systolic dimensions indicate improved wall motion after Tat-Beclin treatment which correlate with our observations of robust infarct size reduction. The ability of this peptide to protect against reperfusion injury correlates with an increase in cardiomyocyte autophagy in the infarct border zone.

Findings reported here clearly suggest that inducing autophagic flux is sufficient to protect the heart from I/R injury. However, there still remained a question whether the autophagy-inducing peptide, Tat-Beclin, had some unknown effects due to non-specific actions. We therefore tested whether loss of ATG7, an essential autophagy-related protein, blocks Tat-Beclin's protective effects. In mice harboring a cardiomyocyte-specific deficiency in ATG7, the protective effects of Tat-Beclin peptide are lost, which confirms that Tat-Beclin's protective effect occurs through bona fide activation of autophagy. Further, these data are consistent with earlier reports from our laboratory that highlighted a similar increase in autophagy, triggered by HDAC inhibition, as the driving force behind the protection observed¹⁵. Our study of an autophagy-deficient mouse model (cardiomyocyte-specific ATG7 knockout mice) provides direct *in vivo* evidence for the cardioprotective benefit of autophagy under these conditions.

Although there is a report of a baseline heart failure phenotype in ATG7 knockout mice⁴⁷, we did not detect significant systolic dysfunction five days after the induction of mer-Cre-mer with our injection protocol. Tamoxifen-induced contractile dysfunction is dependent on dosage; our study employed 20mg/kg IP for five days, and we did not observe these changes. By contrast, the other study used 225mg/kg IP for seven days which likely accounts for these differences⁴⁷.

Of note, TAT-Beclin has a relatively narrow therapeutic window. This may be due to the fact that maintaining autophagic homeostasis is essential for basal cardiomyocyte function, and that over-activation (or over-suppression) of autophagy promotes pathologic cardiac remodeling⁴⁸. This fact should be considered when designing a possible clinical trial.

Mechanisms underlying autophagy's cardioprotective effects are likely through ROS reduction, mitochondrial homeostasis, and energy production.

The initial trigger of reperfusion injury is believed to derive from a burst of ROS from mitochondria immediately upon restoration of normoxic conditions⁸. This mitochondrial ROS production elicits acute damage, as well as initiates subsequent pathology that develops over time. Oxidative damage to mitochondria can lead to decreased ATP production, activation of the mitochondrial permeability transition pore, and release of mtDNA that can act as damage-associated molecular pattern molecules and trigger a sterile inflammatory response⁴⁹. Whereas detailed mechanisms whereby induction of autophagy protects against reperfusion injury remain unclear, it is generally accepted that mitochondrial dysfunction and the production of ROS are central drivers of cardiomyocyte death under these conditions¹². Here, we present evidence that induction of cardiomyocyte autophagy in the border zone leads to a decrease in oxidative stress. This, in return, may result in a decrease in cell death, thus limiting infarct size.

Autophagy is known to target damaged mitochondria in a process known as mitophagy^{40, 43, 50}. Whereas mitophagy is a targeted process, here we induced macroautophagy, a generalized form of intracellular recycling. Of note, recent work has identified an alternative mitophagy pathway independent of ATG7 and the macroautophagy stimulated here that protects the heart against ischemia⁵¹. Whether upregulation of ATG7-dependent autophagy results in increased mitophagy, or whether generalized increases in nonspecific autophagy help clear damaged mitochondria, remains to be determined.

Turnover of dysfunctional mitochondria may not be the key mechanism underlying the benefit conferred by increased autophagic flux acutely. Other possibilities include increased turnover of damaged and cytotoxic proteins and aggregates or a more direct metabolic effect through the provision of metabolites. Additionally, the acute nature of the autophagy stimulation (a single treatment at the time of reperfusion) may be an important factor, as persistent autophagic stimulation can exacerbate pathological remodeling under some conditions⁵². However, hours after reperfusion, mitochondrial homeostasis may play some role in long-term cardiomyocyte survival and recovery of function. A recent study reported that HDAC inhibition's cardioprotective effects on mitochondria depend both on autophagy and PGC1 α -dependent mitochondrial biogenesis⁵³.

Conclusion and perspective.

Tat-Beclin, a novel and powerful autophagy-inducing peptide, has afforded the means of manipulating autophagy to define mechanisms underlying cardioprotective autophagic flux and elucidate how autophagy is beneficial in the setting of reperfusion injury. The narrow therapeutic window of Tat-Beclin signifies the importance of maintaining appropriate activation of autophagic flux while not triggering damage^{12, 54}. In addition, it holds promise as a therapeutic agent to reduce cardiovascular mortality due to I/R injury in the clinical setting. It is noteworthy that activation of autophagic flux in cardiomyocytes is both mTOR-dependent¹⁵ and mTOR-independent (this report) mechanisms affords similar degrees of cardioprotection. Looking to the future, therapeutic interventions to limit infarct size, such

as HDAC inhibition or Tat-Beclin administration at the time of reperfusion, may emerge as clinically relevant interventions¹⁸.

Supplementary Material

Refer to Web version on PubMed Central for supplementary material.

SOURCES OF FUNDING

This work was supported by grants from NIH: HL-120732 (J.A.H.), HL-128215 (J.A.H.), HL-126012 (J.A.H.), HL-147933 (J.A.H.), HL-155765 (J.A.H.), American Heart Association (AHA): 14SFRN20510023 (J.A.H.), 14SFRN20670003 (J.A.H.), AHA 15POST22670003 (G.W.C), NIH T32-98040-4/5 (G.W.C), NIH K08-HL127305 (M.X.), R03-HL141620 (M.X.), HL153501 (M.X.), AHA and the Theodore and Beulah Beasley Foundation 18POST34060230 (G.G.S.), AHA Postdoctoral fellowship 16POST30680016 (F.A.), University Federico II of Naples and Compagnia di San Paolo STAR program (G.G.S.).

Nonstandard Abbreviations and Acronyms:

HDACs	histone deacetylases
HDACi	HDAC inhibition
TB	Tat-Beclin 1
TS	Tat-Scrambled
SAHA	suberanilohydroxamic acid
DMSO	dimethyl sulfoxide
ATG7^{F/F}	ATG7 floxed allele
ATG7 KO	ATG7 knockout mice

REFERENCES

1. Moran AE, Forouzanfar MH, Roth GA, Mensah GA, Ezzati M, Murray CJ, Naghavi M. Temporal trends in ischemic heart disease mortality in 21 world regions, 1980 to 2010: The global burden of disease 2010 study. *Circulation*. 2014;129:1483–1492 [PubMed: 24573352]
2. Yusuf S, Joseph P, Rangarajan S, Islam S, Mentz A, Hystad P, Brauer M, Kutty VR, Gupta R, Wielgosz A, AlHabib KF, Dans A, Lopez-Jaramillo P, Avezum A, Lanas F, Oguz A, Kruger IM, Diaz R, Yusuf K, Mony P, Chifamba J, Yeates K, Kelishadi R, Yusufali A, Khatib R, Rahman O, Zatonska K, Iqbal R, Wei L, Bo H, Rosengren A, Kaur M, Mohan V, Lear SA, Teo KK, Leong D, O'Donnell M, McKee M, Dagenais G. Modifiable risk factors, cardiovascular disease, and mortality in 155 722 individuals from 21 high-income, middle-income, and low-income countries (pure): A prospective cohort study. *Lancet*. 2020;395:795–808 [PubMed: 31492503]
3. Virani SS, Alonso A, Benjamin EJ, Bittencourt MS, Callaway CW, Carson AP, Chamberlain AM, Chang AR, Cheng S, Delling FN, Djousse L, Elkind MSV, Ferguson JF, Fornage M, Khan SS, Kissela BM, Knutson KL, Kwan TW, Lackland DT, Lewis TT, Lichtman JH, Longenecker CT, Loop MS, Lutsey PL, Martin SS, Matsushita K, Moran AE, Mussolino ME, Perak AM, Rosamond WD, Roth GA, Sampson UKA, Satou GM, Schroeder EB, Shah SH, Shay CM, Spartano NL, Stokes A, Tirschwell DL, VanWagner LB, Tsao CW, American Heart Association Council on E, Prevention Statistics C, Stroke Statistics S. Heart disease and stroke statistics-2020 update: A report from the American Heart Association. *Circulation*. 2020;141:e139–e596 [PubMed: 31992061]

4. Braunwald E, Morrow DA. Unstable angina: Is it time for a requiem? *Circulation*. 2013;127:2452–2457 [PubMed: 23775194]
5. Giugliano RP, Braunwald E. The year in acute coronary syndrome. *Journal of the American College of Cardiology*. 2014;63:201–214 [PubMed: 24239661]
6. Altamirano F, Wang ZV, Hill JA. Cardioprotection in ischaemia-reperfusion injury: Novel mechanisms and clinical translation. *J Physiol*. 2015;593:3773–3788 [PubMed: 26173176]
7. Cho GW, Altamirano F, Hill JA. Chronic heart failure: Ca(2+), catabolism, and catastrophic cell death. *Biochimica et biophysica acta*. 2016;1862:763–777 [PubMed: 26775029]
8. Hausenloy DJ, Yellon DM. Ischaemic conditioning and reperfusion injury. *Nat Rev Cardiol*. 2016;13:193–209 [PubMed: 26843289]
9. Turer AT, Hill JA. Pathogenesis of myocardial ischemia-reperfusion injury and rationale for therapy. *The American journal of cardiology*. 2010;106:360–368 [PubMed: 20643246]
10. Bulluck H, Yellon DM, Hausenloy DJ. Reducing myocardial infarct size: Challenges and future opportunities. *Heart (British Cardiac Society)*. 2016;102:341–348 [PubMed: 26674987]
11. Hausenloy DJ, Yellon DM. Targeting myocardial reperfusion injury--the search continues. *The New England journal of medicine*. 2015;373:1073–1075 [PubMed: 26321104]
12. Kloner RA, Brown DA, Csete M, Dai W, Downey JM, Gottlieb RA, Hale SL, Shi J. New and revisited approaches to preserving the reperfused myocardium. *Nat Rev Cardiol*. 2017;14:679–693 [PubMed: 28748958]
13. Granger A, Abdullah I, Huebner F, Stout A, Wang T, Huebner T, Epstein JA, Gruber PJ. Histone deacetylase inhibition reduces myocardial ischemia-reperfusion injury in mice. *FASEB journal : official publication of the Federation of American Societies for Experimental Biology*. 2008;22:3549–3560 [PubMed: 18606865]
14. Kessler-Ickeson G, Hochhauser E, Sinai T, Kremer A, Dick J, Tarasenko N, Nudelman V, Schlesinger H, Abraham S, Nudelman A, Rephaeli A. A histone deacetylase inhibitory prodrug - butyroyloxymethyl diethyl phosphate - protects the heart and cardiomyocytes against ischemia injury. *European journal of pharmaceutical sciences : official journal of the European Federation for Pharmaceutical Sciences*. 2012;45:592–599 [PubMed: 22234377]
15. Xie M, Kong Y, Tan W, May H, Battiprolu PK, Pedrozo Z, Wang ZV, Morales C, Luo X, Cho G, Jiang N, Jessen ME, Warner JJ, Lavandero S, Gillette TG, Turer AT, Hill JA. Histone deacetylase inhibition blunts ischemia/reperfusion injury by inducing cardiomyocyte autophagy. *Circulation*. 2014;129:1139–1151 [PubMed: 24396039]
16. Zhang Y, Ren J. Targeting autophagy for the therapeutic application of histone deacetylase inhibitors in ischemia/reperfusion heart injury. *Circulation*. 2014;129:1088–1091 [PubMed: 24396040]
17. Wang J, Hu X, Jiang H. Hdac inhibition: A novel therapeutic target for attenuating myocardial ischemia and reperfusion injury by reversing cardiac remodeling. *Int J Cardiol*. 2015;190:126–127 [PubMed: 25918063]
18. Xie M, Tang Y, Hill JA. Hdac inhibition as a therapeutic strategy in myocardial ischemia/reperfusion injury. *Journal of molecular and cellular cardiology*. 2019;129:188–192 [PubMed: 30825484]
19. Yang J, He J, Ismail M, Tweeten S, Zeng F, Gao L, Ballinger S, Young M, Prabhu SD, Rowe GC, Zhang J, Zhou L, Xie M. Hdac inhibition induces autophagy and mitochondrial biogenesis to maintain mitochondrial homeostasis during cardiac ischemia/reperfusion injury. *J Mol Cell Cardiol*. 2019;130:36–48 [PubMed: 30880250]
20. Cao DJ, Wang ZV, Battiprolu PK, Jiang N, Morales CR, Kong Y, Rothermel BA, Gillette TG, Hill JA. Histone deacetylase (hdac) inhibitors attenuate cardiac hypertrophy by suppressing autophagy. *Proceedings of the National Academy of Sciences of the United States of America*. 2011;108:4123–4128 [PubMed: 21367693]
21. Kong Y, Tannous P, Lu G, Berenji K, Rothermel BA, Olson EN, Hill JA. Suppression of class i and ii histone deacetylases blunts pressure-overload cardiac hypertrophy. *Circulation*. 2006;113:2579–2588 [PubMed: 16735673]
22. Morales CR, Li DL, Pedrozo Z, May HI, Jiang N, Kyrychenko V, Cho GW, Kim SY, Wang ZV, Rotter D, Rothermel BA, Schneider JW, Lavandero S, Gillette TG, Hill JA. Inhibition of class i

- histone deacetylases blunts cardiac hypertrophy through tsc2-dependent mtor repression. *Science signaling*. 2016;9:ra34 [PubMed: 27048565]
23. Lavandero S, Chiong M, Rothermel BA, Hill JA. Autophagy in cardiovascular biology. *The Journal of clinical investigation*. 2015;125:55–64 [PubMed: 25654551]
 24. Morales CR, Pedrozo Z, Lavandero S, Hill JA. Oxidative stress and autophagy in cardiovascular homeostasis. *Antioxidants & redox signaling*. 2014;20:507–518 [PubMed: 23641894]
 25. Schiattarella GG, Hill JA. Therapeutic targeting of autophagy in cardiovascular disease. *J Mol Cell Cardiol*. 2015
 26. Wang ZV, Hill JA. Protein quality control and metabolism: Bidirectional control in the heart. *Cell metabolism*. 2015;21:215–226 [PubMed: 25651176]
 27. Haberland M, Montgomery RL, Olson EN. The many roles of histone deacetylases in development and physiology: Implications for disease and therapy. *Nat Rev Genet*. 2009;10:32–42 [PubMed: 19065135]
 28. Mahmoodzadeh S, Fliegner D, Dworatzek E. Sex differences in animal models for cardiovascular diseases and the role of estrogen. *Handbook of experimental pharmacology*. 2012:23–48
 29. Li D, Wu J, Bai Y, Zhao X, Liu L. Isolation and culture of adult mouse cardiomyocytes for cell signaling and in vitro cardiac hypertrophy. *J Vis Exp*. 2014
 30. Shoji-Kawata S, Sumpter R, Leveno M, Campbell GR, Zou Z, Kinch L, Wilkins AD, Sun Q, Pallauf K, MacDuff D, Huerta C, Virgin HW, Helms JB, Eerland R, Tooze SA, Xavier R, Lenschow DJ, Yamamoto A, King D, Lichtarge O, Grishin NV, Spector SA, Kaloyanova DV, Levine B. Identification of a candidate therapeutic autophagy-inducing peptide. *Nature*. 2013;494:201–206 [PubMed: 23364696]
 31. Komatsu M, Waguri S, Ueno T, Iwata J, Murata S, Tanida I, Ezaki J, Mizushima N, Ohsumi Y, Uchiyama Y, Kominami E, Tanaka K, Chiba T. Impairment of starvation-induced and constitutive autophagy in atg7-deficient mice. *The Journal of cell biology*. 2005;169:425–434 [PubMed: 15866887]
 32. Sohail DS, Nghiem M, Crackower MA, Witt SA, Kimball TR, Tymitz KM, Penninger JM, Molkentin JD. Temporally regulated and tissue-specific gene manipulations in the adult and embryonic heart using a tamoxifen-inducible cre protein. *Circulation research*. 2001;89:20–25 [PubMed: 11440973]
 33. Sciarretta S, Volpe M, Sadoshima J. Mammalian target of rapamycin signaling in cardiac physiology and disease. *Circulation research*. 2014;114:549–564 [PubMed: 24481845]
 34. Sciarretta S, Zhai P, Shao D, Maejima Y, Robbins J, Volpe M, Condorelli G, Sadoshima J. Rheb is a critical regulator of autophagy during myocardial ischemia: Pathophysiological implications in obesity and metabolic syndrome. *Circulation*. 2012;125:1134–1146 [PubMed: 22294621]
 35. Xie M, Hill JA. Hdac-dependent ventricular remodeling. *Trends in cardiovascular medicine*. 2013;23:229–235 [PubMed: 23499301]
 36. Khan S, Salloum F, Das A, Xi L, Vetrovec GW, Kukreja RC. Rapamycin confers preconditioning-like protection against ischemia-reperfusion injury in isolated mouse heart and cardiomyocytes. *J Mol Cell Cardiol*. 2006;41:256–264 [PubMed: 16769083]
 37. Granger DN, Kvietys PR. Reperfusion injury and reactive oxygen species: The evolution of a concept. *Redox biology*. 2015;6:524–551 [PubMed: 26484802]
 38. Neri M, Fineschi V, Di Paolo M, Pomara C, Riezzo I, Turillazzi E, Cerretani D. Cardiac oxidative stress and inflammatory cytokines response after myocardial infarction. *Current vascular pharmacology*. 2015;13:26–36 [PubMed: 23628007]
 39. Tian PG, Jiang ZX, Li JH, Zhou Z, Zhang QH. Spliced xbp1 promotes macrophage survival and autophagy by interacting with beclin-1. *Biochemical and biophysical research communications*. 2015;463:518–523 [PubMed: 26026678]
 40. Sverdllov AL, Elezaby A, Qin F, Behring JB, Luptak I, Calamaras TD, Siwik DA, Miller EJ, Liesa M, Shirihai OS, Pimentel DR, Cohen RA, Bachschmid MM, Colucci WS. Mitochondrial reactive oxygen species mediate cardiac structural, functional, and mitochondrial consequences of diet-induced metabolic heart disease. *J Am Heart Assoc*. 2016;5

41. Fedorova M, Bollineni RC, Hoffmann R. Protein carbonylation as a major hallmark of oxidative damage: Update of analytical strategies. *Mass spectrometry reviews*. 2014;33:79–97 [PubMed: 23832618]
42. Wang ZV, Deng Y, Gao N, Pedrozo Z, Li DL, Morales CR, Criollo A, Luo X, Tan W, Jiang N, Lehrman MA, Rothermel BA, Lee AH, Lavandero S, Mammen PP, Ferdous A, Gillette TG, Scherer PE, Hill JA. Spliced x-box binding protein 1 couples the unfolded protein response to hexosamine biosynthetic pathway. *Cell*. 2014;156:1179–1192 [PubMed: 24630721]
43. Delbridge LM, Mellor KM, Taylor DJ, Gottlieb RA. Myocardial autophagic energy stress responses--macroautophagy, mitophagy, and glycopagy. *Am J Physiol Heart Circ Physiol*. 2015;308:H1194–1204 [PubMed: 25747748]
44. Zheng Y, Li X, Wang J, Tan J, Zhang C, Yang H. Berberine postconditioning protects the heart from ischemia/reperfusion injury through the regulation of autophagy during reperfusion. *Circulation research*. 2015;117:A257–A257
45. Song H, Yan C, Tian X, Zhu N, Li Y, Liu D, Liu Y, Liu M, Peng C, Zhang Q, Gao E, Han Y. Creg protects from myocardial ischemia/reperfusion injury by regulating myocardial autophagy and apoptosis. *Biochimica et biophysica acta*. 2016
46. Lindsey ML, Kassiri Z, Virag JAI, de Castro Bras LE, Scherrer-Crosbie M. Guidelines for measuring cardiac physiology in mice. *Am J Physiol Heart Circ Physiol*. 2018;314:H733–H752 [PubMed: 29351456]
47. Li S, Liu C, Gu L, Wang L, Shang Y, Liu Q, Wan J, Shi J, Wang F, Xu Z, Ji G, Li W. Autophagy protects cardiomyocytes from the myocardial ischaemia-reperfusion injury through the clearance of clp36. *Open Biol*. 2016;6
48. Rothermel BA, Hill JA. Myocyte autophagy in heart disease: Friend or foe? *Autophagy*. 2007;3:632–634 [PubMed: 17786025]
49. Chouchani ET, Pell VR, James AM, Work LM, Saeb-Parsy K, Frezza C, Krieg T, Murphy MP. A unifying mechanism for mitochondrial superoxide production during ischemia-reperfusion injury. *Cell metabolism*. 2016;23:254–263 [PubMed: 26777689]
50. Vasquez-Trincado C, Garcia-Carvajal I, Pennanen C, Parra V, Hill JA, Rothermel BA, Lavandero S. Mitochondrial dynamics, mitophagy and cardiovascular disease. *J Physiol*. 2016;594:509–525 [PubMed: 26537557]
51. Saito T, Nah J, Oka SI, Mukai R, Monden Y, Maejima Y, Ikeda Y, Sciarretta S, Liu T, Li H, Baljinnyam E, Fraidenraich D, Fritzky L, Zhai P, Ichinose S, Isobe M, Hsu CP, Kundu M, Sadoshima J. An alternative mitophagy pathway mediated by rab9 protects the heart against ischemia. *The Journal of clinical investigation*. 2019;129:802–819 [PubMed: 30511961]
52. Zhu H, Tannous P, Johnstone JL, Kong Y, Shelton JM, Richardson JA, Le V, Levine B, Rothermel BA, Hill JA. Cardiac autophagy is a maladaptive response to hemodynamic stress. *The Journal of clinical investigation*. 2007;117:1782–1793 [PubMed: 17607355]
53. Yang J, He J, Ismail M, Tweeten S, Zeng F, Gao L, Ballinger S, Young M, Prabhu SD, Rowe GC, Zhang J, Zhou L, Xie M. Hdac inhibition induces autophagy and mitochondrial biogenesis to maintain mitochondrial homeostasis during cardiac ischemia/reperfusion injury. *J Mol Cell Cardiol*. 2019
54. Xie M, Morales CR, Lavandero S, Hill JA. Tuning flux: Autophagy as a target of heart disease therapy. *Current opinion in cardiology*. 2011;26:216–222 [PubMed: 21415729]

NOVELTY AND SIGNIFICANCE

What Is Known?

- Histone deacetylase inhibitor (HDACi), SAHA, reduces infarct size when given at reperfusion in mice and rabbits.
- SAHA maintains autophagic flux at the infarct border zone.
- SAHA protects cardiomyocytes from ischemia/reperfusion (I/R) injury through maintaining autophagic flux.

What New Information Does This Article Contribute?

- Autophagy inducing Tat-Beclin peptide reduces infarct size to the same extent as SAHA when given at the time of reperfusion in mice.
- Tat-Beclin's cardiac protective effects depend on the essential autophagy gene, ATG7.
- Tat-Beclin protects cardiomyocytes by inducing autophagic flux and reducing reactive oxygen species.

Although SAHA induces autophagy in the myocardium, whether inducing autophagy alone protects the myocardium when given at the time of reperfusion is unknown. This study showed that inducing autophagy at the reperfusion alone is cardioprotective. These findings build a foundation to develop novel therapeutics to mitigate reperfusion injury through inducing autophagy in cardiomyocytes.

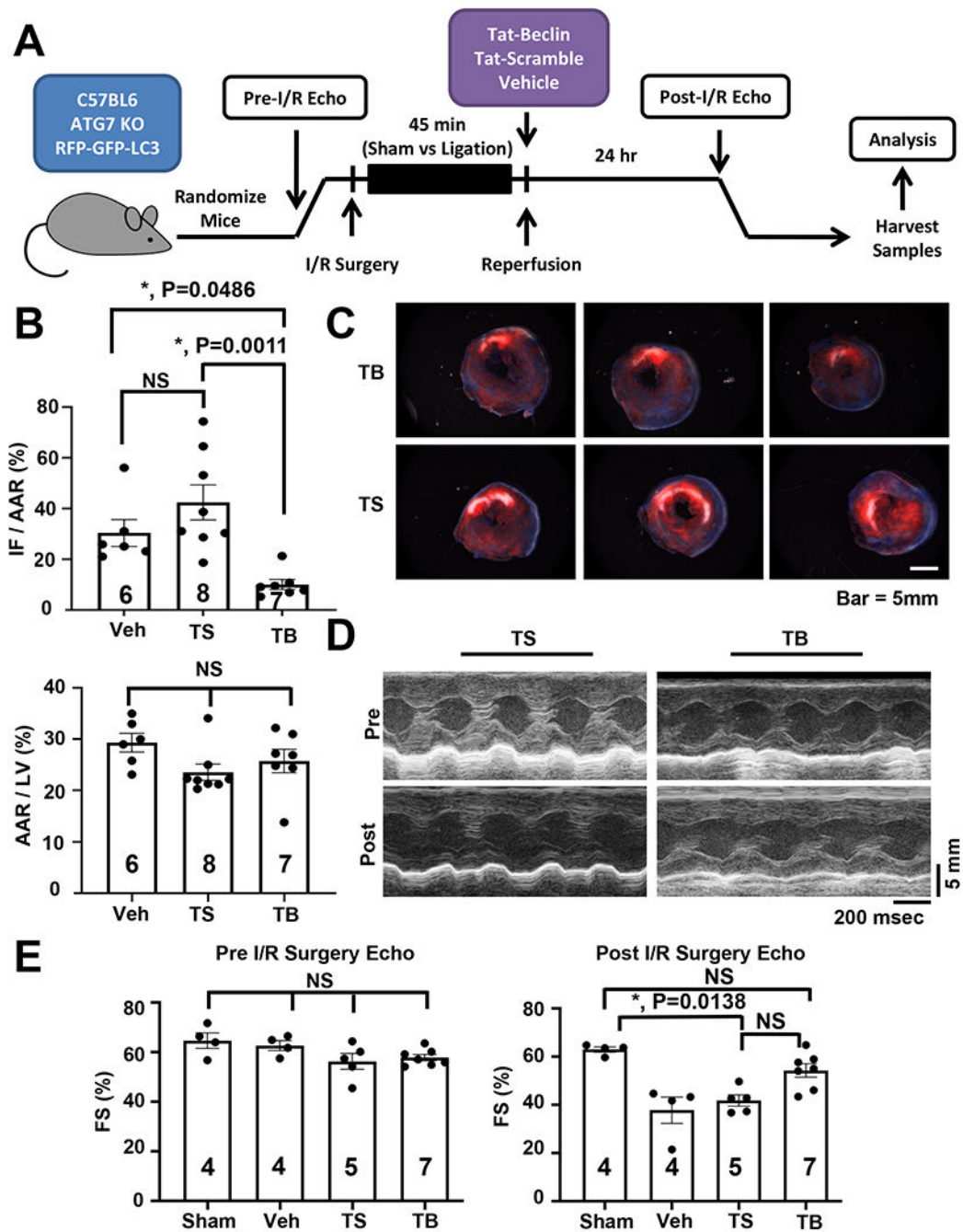


Figure 1. Tat-Beclin peptide rescues cardiac I/R injury *in vivo*.

(A) Schematic of *in vivo* simulated I/R injury model and experimental protocol. (B) Quantification of TTC staining delineating infarct size (IF – infarct, AAR – area at risk, LV – left ventricle) showing reduction of I/R injury with Tat-Beclin administration. N = 6-8, P = 0.0011. (C) Representative cardiac TTC staining histology demonstrating reduction of infarct size with Tat-Beclin treatment. (D) Representative M-mode echocardiogram images. (E) Quantification of cardiac function based on echocardiography (FS – fractional shortening) showing preservation of systolic function in mice receiving Tat-Beclin peptide at

reperfusion. Kruskal-Wallis test with Dunn's multiple comparisons test was used in all panel. Sham vs. TS, $P = 0.001$; Sham vs. TB, $P = \text{NS}$; TS vs. TB, $P = \text{NS}$ (results of one-way ANOVA followed by Tukey's multiple comparisons test: I/R Veh vs. SAHA, $P = 0.0001$).

Author Manuscript

Author Manuscript

Author Manuscript

Author Manuscript

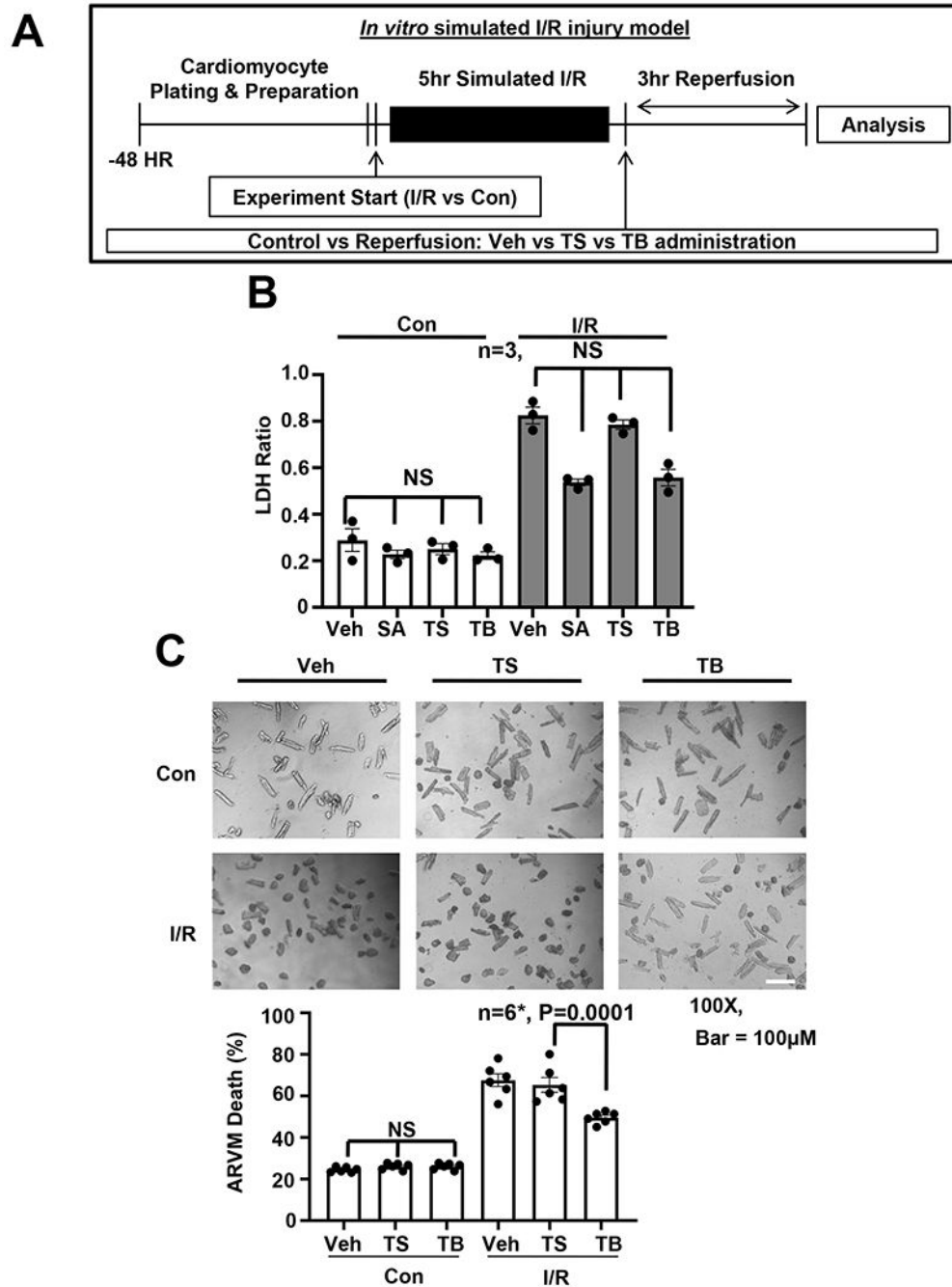


Figure 2. Tat-Beclin rescues cardiomyocyte cell death *in vitro*.

(A) Schematic of *in vitro* simulated I/R injury model and experimental protocol. (B) LDH cell death assay evaluating NRVM treatment with vehicle, SAHA [2 μ M], TS [2.5 μ M] or TB [2.5 μ M] in control and simulated I/R conditions, showing reduction of I/R induced cell death with SAHA and TB treatment. N = 3 with consistent results, Results of Kruskal-Wallis test with Dunn's multiple comparisons test depicted in figure. (C) ARVM microscopy and quantification showing improved I/R cell survival with TB treatment. All samples

normalized to control protein standard. Passed normality test. One-way ANOVA followed by Tukey's multiple comparisons test was used: $N = 6$, $P = 0.0001$.

Author Manuscript

Author Manuscript

Author Manuscript

Author Manuscript

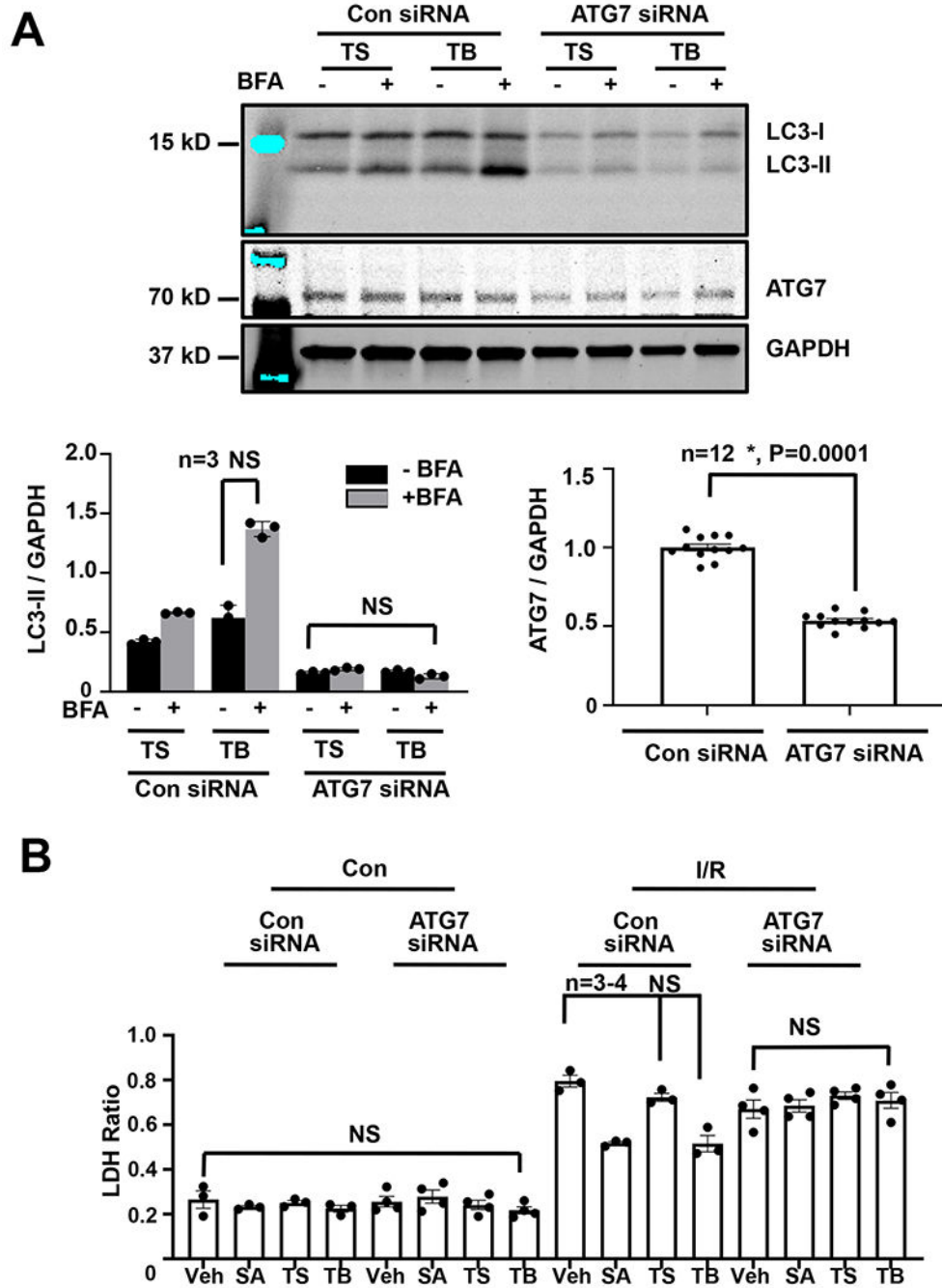


Figure 3. Tat-Beclin rescue of I/R Injury *in vitro* is lost with autophagy inhibition. (A) Immunoblot detection and quantification of ATG7 and LC3 levels normalized to GAPDH extracted from NRVMs showing that SAHA and TB treatment increases autophagic flux, which is lost with ATG7 knockdown. N = 3 with consistent results. results of Kruskal-Wallis test with Dunn’s multiple comparisons test depicted in figure). (B) LDH cell death assay evaluating NRVM treatment with vehicle, SAHA [2 μM], TS [2.5 μM] or TB [2.5 μM] in control and simulated I/R conditions, showing that SAHA and TB peptide’s ability to rescue I/R injury is lost with autophagy inhibition with siATG7. N = 3 with

consistent results. Results of Kruskal-Wallis test with Dunn's multiple comparisons test depicted in figure.

Author Manuscript

Author Manuscript

Author Manuscript

Author Manuscript

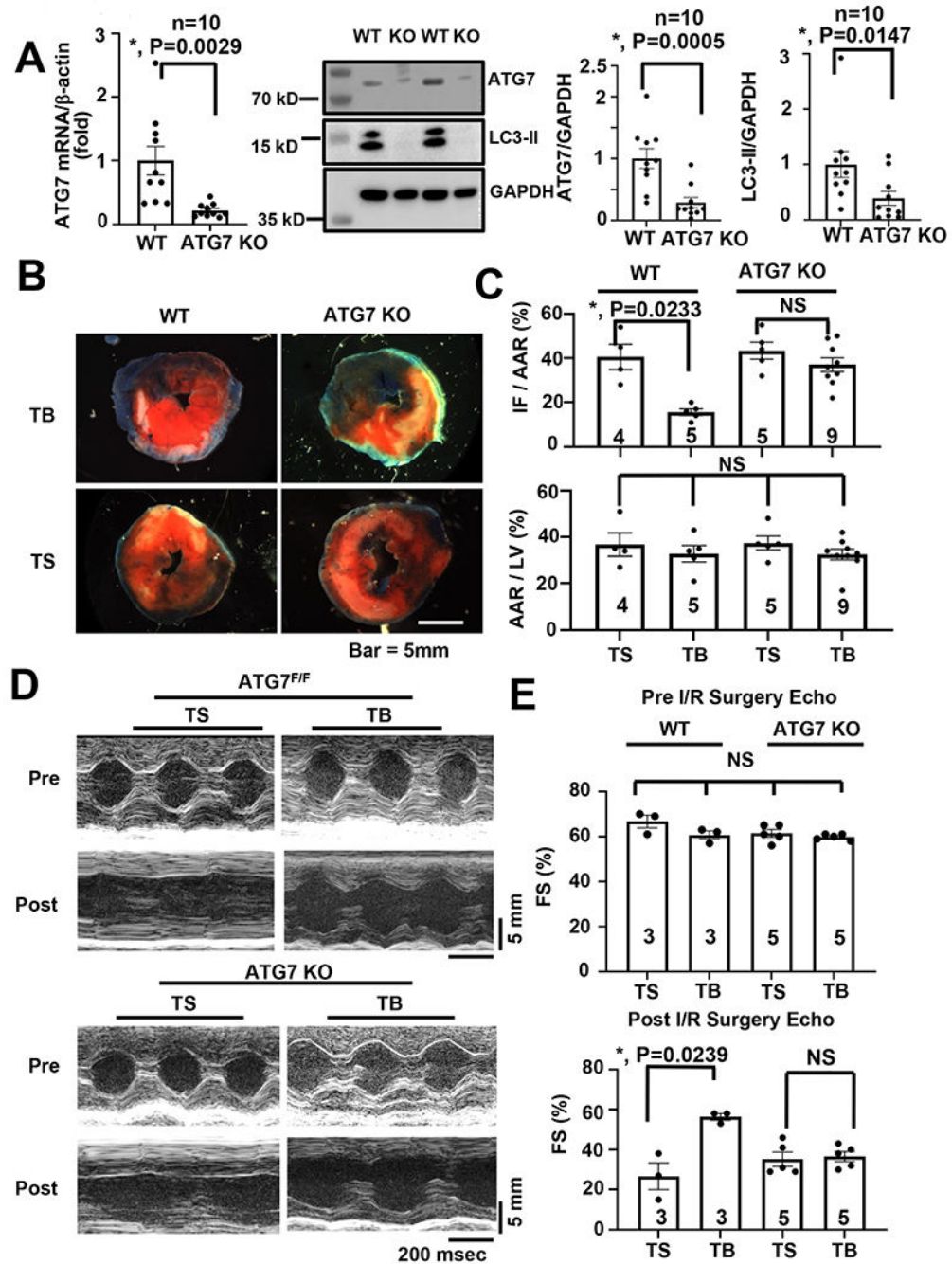


Figure 4. Tat-Beclin fails to rescue cardiac I/R injury with the loss of autophagy.

(A) ATG7 is successfully knocked out in cardiomyocytes. Left: qRT-PCR of mouse ATG7 mRNA normalized to β -actin in isolated adult mouse cardiomyocytes. Middle: Western blots of ATG7 and LC3. Right: Quantification. The wild-type group was normalized to one. $N = 10$, $P < 0.015$ in all groups. (B) Representative cardiac TTC staining histology demonstrating that reduction of infarct size with TB treatment is abrogated in mice with cardiac deficiency of the autophagy protein ATG7. (C) Quantification of TTC staining delineating infarct size demonstrating that I/R injury rescue with TB administration is lost in

ATG7 cardiomyocyte specific KO mice. N = 4-9, P = 0.0233. (D) Representative M-mode echocardiogram images pre/post operation in both ATG7^{F/F} and KO groups. (E) Quantification of contractile function demonstrating preservation of systolic function only in ATG7^{F/F} mice receiving TB peptide at reperfusion versus no differences observed in ATG7 KO mice between TS or TB administration. N = 3-5 animals per group, P = 0.0239. Kruskal-Wallis test with Dunn's multiple comparisons test was used in all panel.

Author Manuscript

Author Manuscript

Author Manuscript

Author Manuscript

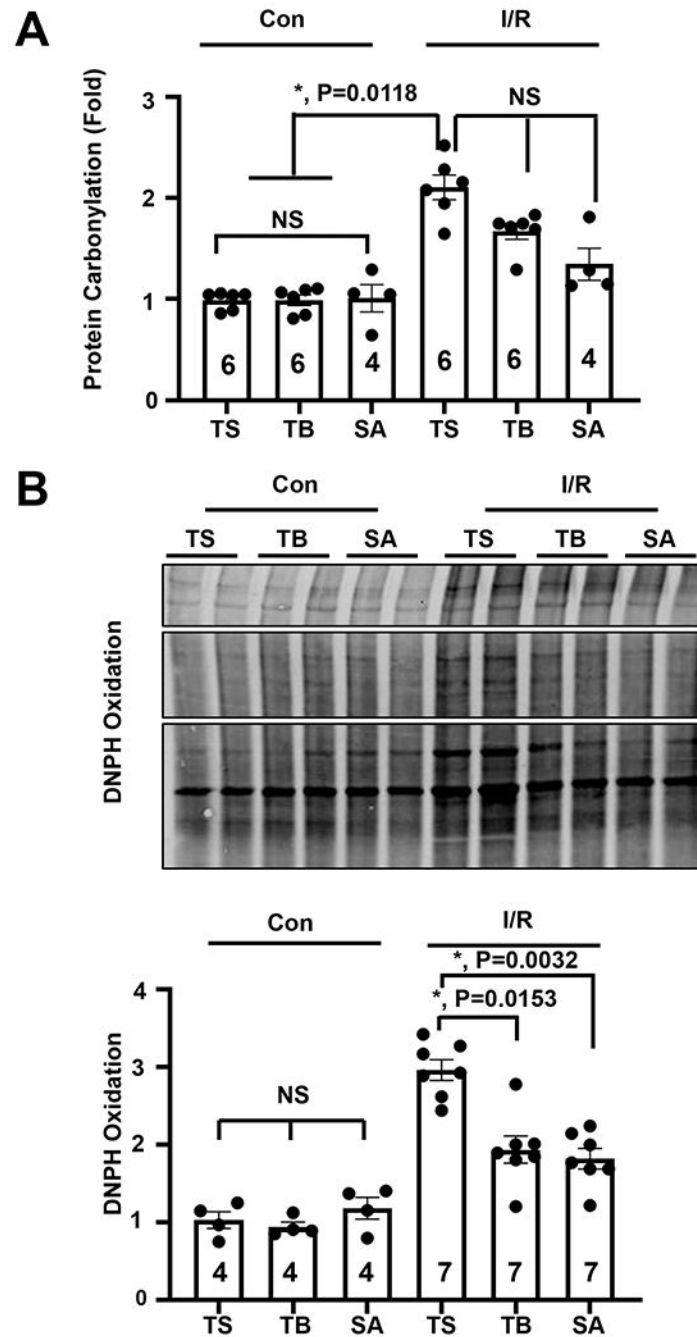


Figure 5. Tat-Beclin and SAHA reduce oxidative stress during I/R injury rescue.

(A) Quantification of oxidative stress measured by luminescence protein carbonylation assay demonstrating reduction of oxidative stress with TB and SAHA administration in NRVMs. N = 4-6 with consistent results. Results of Kruskal-Wallis test with Dunn's multiple comparisons test depicted in (B) Immunoblot detection and quantification of reactive oxygen species levels by DNPH oxidation assay demonstrating ROS reduction with TB and SAHA administration. The control TS group is normalized to one. Kruskal-Wallis test with Dunn's multiple comparisons test was used: I/R TS vs TB, P = 0.0153.

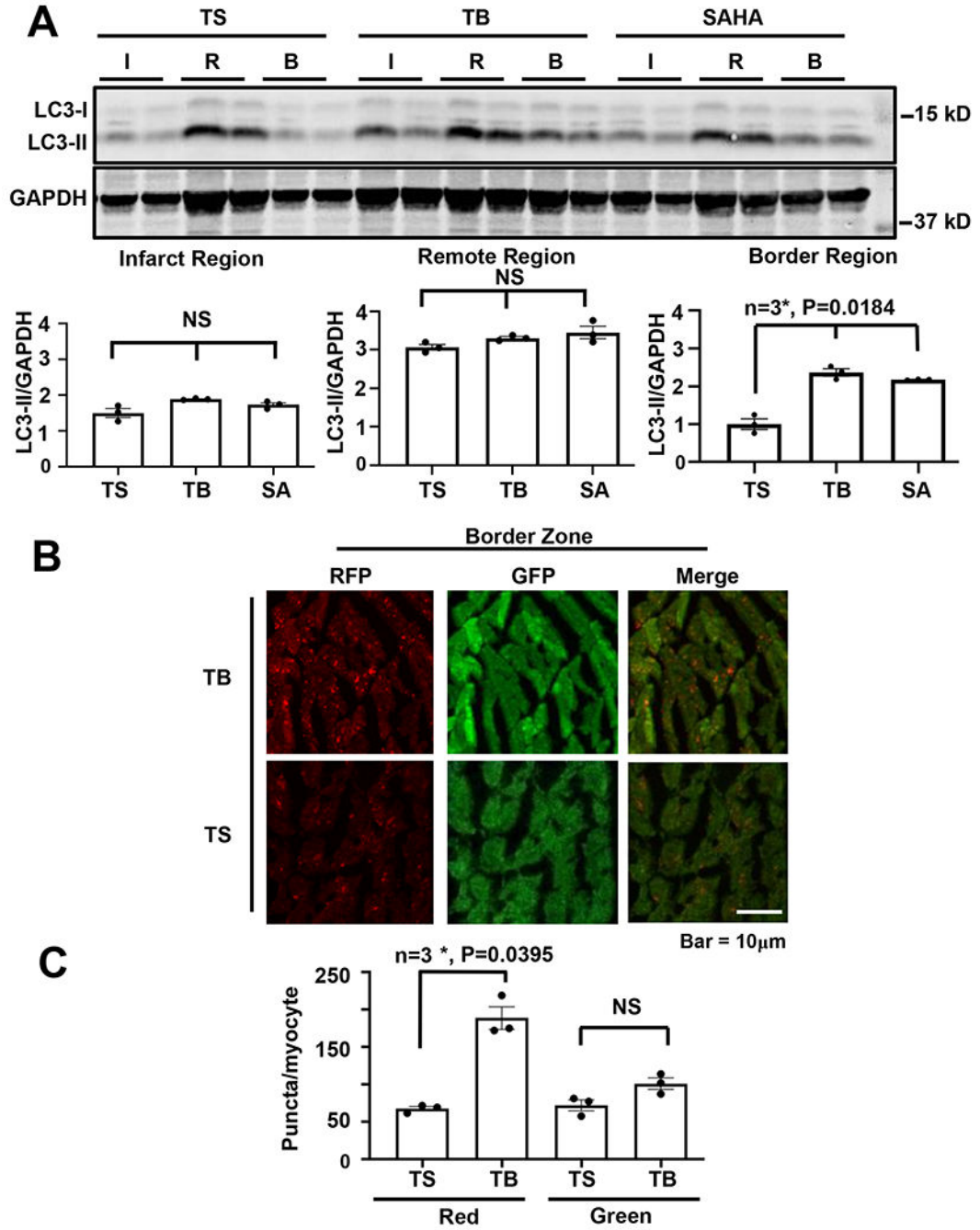


Figure 6. Tat-Beclin increases autophagy at the infarct-border zone during rescue of cardiac I/R injury.

(A) Immunoblot detection and quantification of the LC3 autophagy marker normalized to GAPDH showing preserved autophagy at the border region surrounding the infarct with TB (20mg/kg) or SAHA (100mg/kg) administration, but not observed with TS (20mg/kg). N = 3, P = 0.0184 in border region. The LC3-II level of the TS-treated border region is normalized to one. (B, C) Immunohistochemistry and quantification of the cardiac border region in RFP-GFP-LC3 transgenic mice showing increased autophagic flux by lysosomal

GFP-RFP conversion with TB treatment. $N = 3$, $P = 0.0395$. Kruskal-Wallis test with Dunn's multiple comparisons test was used in all panel.

Author Manuscript

Author Manuscript

Author Manuscript

Author Manuscript

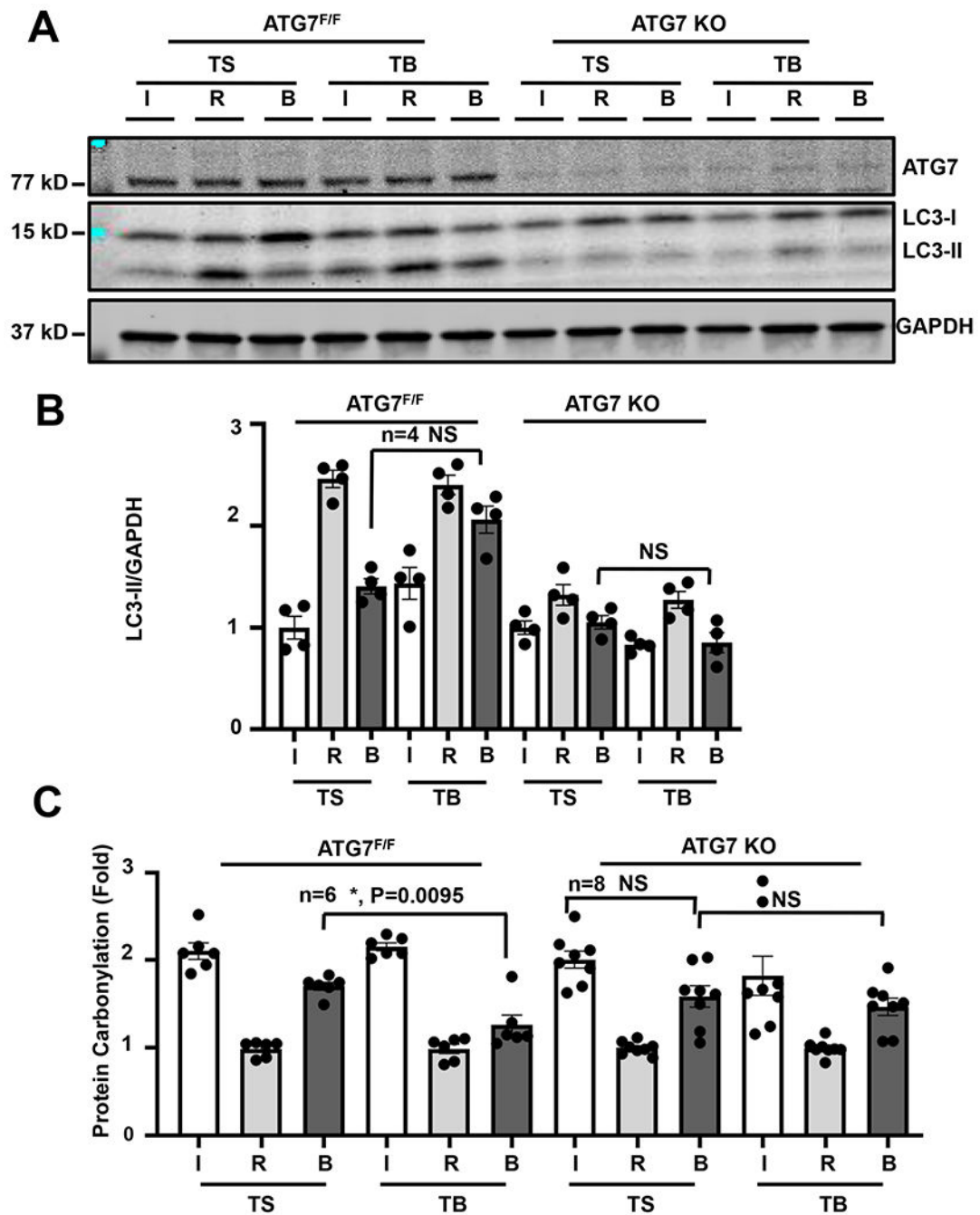


Figure 7. Loss of Tat-Beclin-induced autophagy at the cardiac infarct-border zone in ATG7 KO mice.

(A, B) Immunoblot detection and quantification of the autophagy marker LC3 normalized to GAPDH showing that the preservation of autophagy at the border region surrounding the infarct with TB (20mg/kg) administration is lost in the ATG7 KO cohort. The TS-treated ischemia region is normalized to one. N = 4 with consistent results. Results of Kruskal-Wallis test with Dunn's multiple comparisons test depicted in figure. (C) Quantification of oxidative stress measured by luminescence protein carbonylation assay in heart infarct/ border/remote region samples from ATG7 F/F or KO mice demonstrating reduction of

oxidative stress with TB and SAHA administration at the border region only in ATG7^{F/F} mice, and absence of this reduction in the ATG7 KO cohorts. The remote region of each group is normalized to one. Kruskal-Wallis test with Dunn's multiple comparisons test was used, N = 6, border zone (B), TS vs TB, P = 0.0095.

Author Manuscript

Author Manuscript

Author Manuscript

Author Manuscript